High density mapping systems for SRF cavities

AUTHOR(S):

Fuwa, Yasuhiro; Iwashita, Yoshihisa; Kuriyama, Yasutoshi; Tongu, Hiromu; Hayano, Hitoshi; Geng, R. L.

CITATION:

Fuwa, Yasuhiro ...[et al]. High density mapping systems for SRF cavities. Proceedings of 20th International Conference on RF Superconductivity (SRF 2021) 2022: 323-325

ISSUE DATE:

2022-05-02

20th Int. Conf. on RF Superconductivity SRF2021, East Lansing, MI, USA JACoW Publishing
ISBN: 978-3-95450-233-2 ISSN: 2673-5504 doi:10.18429/JACoW-SRF2021-MOPFDV002

HIGH DENSITY MAPPING SYSTEMS FOR SRF CAVITIES

Y. Fuwa, J-PARC Center, JAEA, Tokai, Ibaraki, Japan
Y. Iwashita, Y. Kuriyama, IIRNS, Kyoto University, Kumatori, Osaka, Japan
H. Tongu, ICR, Kyoto University, Uji, Kyoto, Japan
H. Hayano, KEK, Tsukuba, Ibaraki, Japan
R. L. Geng#, JLab, Newport News, VA, USA

Abstract

High density mapping systems for superconducting RF cavities are prepared. They include sX-map, XT-map, and B-map, which can be used to detect the distribution of X-ray, temperature, and magnetic flux. sX-map is a strip shape detector for X-ray that can be set under stiffener rings of superconducting cavities. Each strip of the sX-map system has 32 X-ray sensors approximately 10 mm apart, which can be inserted under the stiffener rings to show uniform higher sensitivities. This is suitable to get X-ray distribution around iris areas. The XT-map system enables temperature distribution mapping of cavity cells with high spatial resolution at approximately 10 mm intervals in both azimuth and latitude. It also gives X-ray distribution on cells, as well. Magnetic field distributions can be obtained by the B-map system using AMR sensors. Since all these systems are based on the technology of multiplexing at the cryogenic side, fewer wires can carry the huge number of signals. Among the systems, sX-map system is reported.

INTRODUCTION

Inspection equipment for SRF (Superconducting Radio Frequency) cavities during vertical tests is important to evaluate the characteristics of cavities. Active researches are being conducted to achieve high-Q or high-gradient cavities [1], measurement devices with high sensitivity and high positional resolution are needed for us to observe various physical quantities such as local temperature increase, X-ray emission, and trapped magnetic flux [2]. Utilizing high density mapping systems with high sensitivity sensors, source spot of quench or field emission X-ray can be identified with high accuracy. In this article, an overview of the mapping systems and recent results of test experiments on sX-map, an X-ray mapping system for stiffener region, are reported.

HIGH DENSITY MAPPING SYSTEM

Sensors of temperature, X-ray, and trapped magnetic flux are widely used to locate the positions where quench or field emitted X-rays are generated. While a large number of sensors are required to raise the positional resolution of the measurement, the number of lines to read out the signals tends to increase with the number of sensors. As the number of the wires increases, the experimental setup becomes more complicated, and the heat intrusion into the cryostat through the wires increases, which disturb the efficient operation of cavity tests and raise the cost. In order to simplify the connection scheme and to reduce the wires for readout, mapping systems with multiplexers are developed, which can scan a large number of the sensor signals inside the cryogenic dewar. All the active (semiconductor) devices to multiplex, amplify, and convert the signals are CMOS circuits that can work even at the cryogenic temperature. The devices include digital logics and analog multiplexers.

We picked up RuO (Ruthenium Oxide) chip resistors as the cryogenic temperature sensors, infrared photo-diodes as the X-ray sensors, and AMR (Anisotropic Magneto Resistance) flux sensors. Starting from the high-density temperature mapping system [3], 3 types of mapping systems are under development; X-ray mapping system in stiffener region (sX-map), X-ray and Temperature mapping system (XT-map), and magnetic flux mapping system (B-map) [4]. Figure 1 shows prototype systems of sX-map and XT-map. In vertical tests, the equipment shown in Fig. 1 is installed in a cryogenic dewar and communicates with a PC outside of the dewar via small numbers of ribbon cables (Fig. 2).

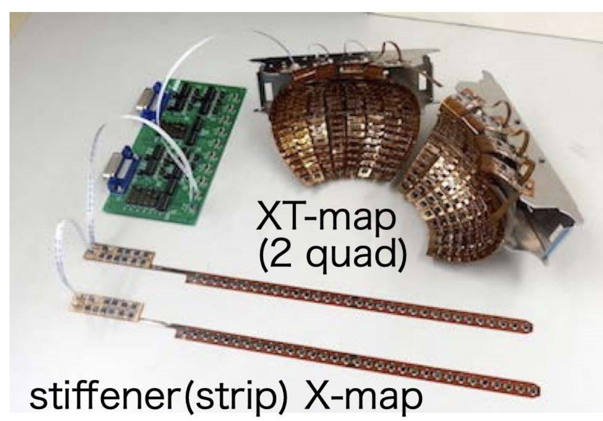

Figure 1: Photo of sX-map and XT-map.

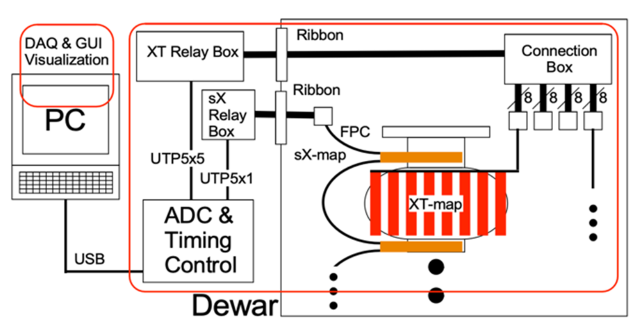

Figure 2: Typical experimental setup of mapping system.

Present Affiliation: Oak Ridge national Laboratory, Oak Ridge, TN, USA

ISBN: 978-3-95450-233-2 ISSN: 2673-5504 doi:10.18429/JACoW-SRF2021-MOPFDV002

sX-map SYSTEM OVERVIEW

sX-map uses sensor strips for X-ray detection that are narrow enough to go under stiffener rings of superconducting cavities. Each strip of the sX-map system has 32 X-ray sensors approximately 10 mm apart, which can show uniform higher sensitivities without attenuation or dilution of X-ray due to stiffener ring. This is suitable to get clear X-ray distribution around iris areas. The sensing device on the sX-map circuit is an infrared photo-diode. Although the signal from the X-ray sensor is a charge generated by pair creation of holes and free electrons in the semiconductor region, the information should be read out as voltage. The charge in the photo-diode is stored by a capacitor during the scan period (typically 100 msec). Each charge captured by a capacitor is collected by an integration amplifier through a multi-input analog switch. The integration amplifier is also a CMOS inverter that can work as an analog amplifier. This inverting amplifier is also used as a buffer amplifier before transmitting the signal to outside of the dewar. The sX-map strips are daisy-chain connected by FFC (Flexible Flat Cable), which is converted to a normal ribbon cable before going outside of dewar. The number of wires in FFC is eight for a system, which consists of clock (D), reset(D), Gain set (D), multiplexed signal(A), two power lines (±5 V), and two ground lines, where (D) and (A) stand for digital and analog signal, respectively. A clock signal supplied from the Data AcQuision (DAQ) unit outside of the Dewar, conducts the multiplexers on the sX-map strips. A buffer amplifier is inserted before sending the analog signal to the DAQ system, whose location is away from the vertical test area. For convenience, LAN cable (so-called UTP cable) can be used for connections.

PERFORMANCE TEST OF sX-map SYSTEM IN VERTICAL TEST

sX-map system was installed for the vertical test of a 9-cell Low Surface Field (LSF9-1) cavity developed at Jefferson Lab [5]. Figure 3 shows the LSF9-1 cavities attached sX-map strips. Eight strips of sX-map are installed under the stiffener ring of eight iris areas of the LSF9-1, and two strips are installed wrapping on the two end beam pipes. Totally, ten strips are installed on the cavity and the strips are connected by FFC as a daisy-chain. Scanned by the multiplexer on each strip circuit sequentially, 320 photo-diodes output the signal of X-ray radiation intensity at the photo-diode positions. In the vertical tests, X-ray signals were detected by sX-map system. Figure 4 shows summed-up X-ray intensity detected by sX-map as a function of time. The X-ray intensity is correlated with the field gradient induced in the cavity. The map of X-ray intensity can be reconstructed from the acquired data (Fig. 5). Each rectangle in the map corresponds photo-diode sensor. Those in the same row are sensors in an iris of the cavity, and those in a column have the same azimuth angle. Areas shown in red indicate hotspots with high X-ray intensity.

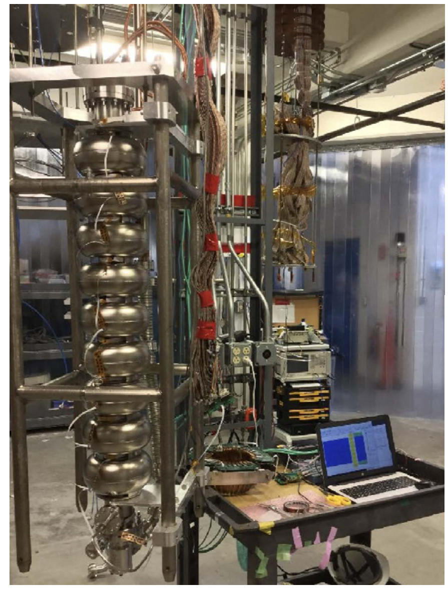

Figure 3: LSF9-1 cavities attached sX-map strips.

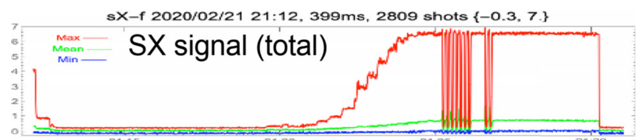

Figure 4: Intensity trend graph of sX-map signal in the vertical test of LSF9-1 cavities.

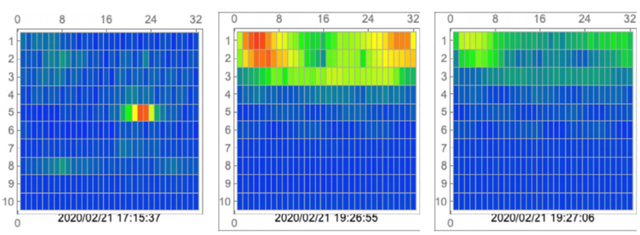

Figure 5: Typical signal distribution from sX-map

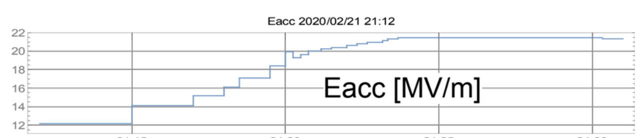

Figure 6: Trend graph of induced gradient inside the LSF9-1 cavity in the vertical test.

Using the data shown in Figs. 4 and 6, plots of I/E_{acc}^2 versus $1/E_{acc}$, *so-called* FN-plot (Fowler-Nordheim plot [6, 7]), can be made to evaluate field emission properties of the cavity. Here, I and E_{acc} correspond to the maximum value of X-ray intensity detected by all photo-diodes on sX-map system and to the cavity gradient at a time in the vertical test, respectively. Figure 7 shows the FN-plot before the big flash events occurred between 21:25 and 21:27 in Fig. 4. Figure 8 shows FN-plot after the events. Among the events, events whose signals are saturated (top left black events in Figs. 7 and 8), are omitted from the fitting. Since the data has an offset, each blue straight line

ISBN: 978-3-95450-233-2 ISSN: 2673-5504 doi:10.18429/JACoW-SRF2021-MOPFDV002

fitting in Fig. 7 and Fig. 8 is performed by omitting events at the bottom right region. The red fitting curves are performed with a fitting function with an additional constant to the regular. For both fitting methods, the field emission coefficient decreases after the flash events, which shows progress of surface processing.

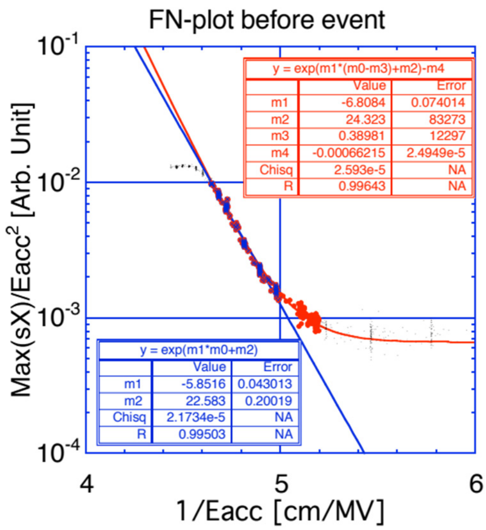

Figure 7: FN-plot before flash events.

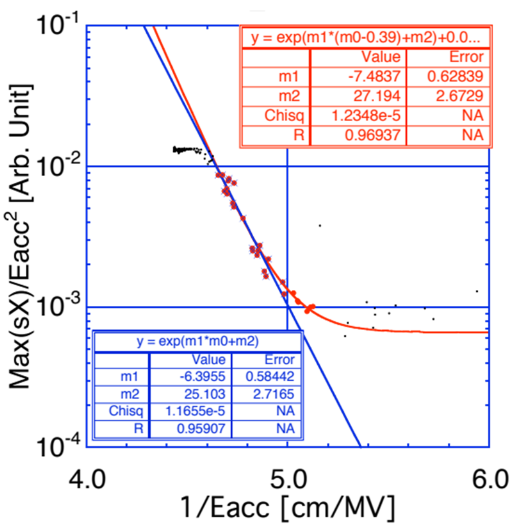

Figure 8: FN-plot after flash events.

CONCLUSION

High density mapping systems for inspection of the SRF cavities are under development. The systems can measure temperature increase, field emission X-ray, and trapped magnetic field on the cavity. As recent progress, a performance test of the sX-map system in a cavity vertical test was carried out and an X-ray signal distribution was successfully detected in the iris region of the cavity.

ACKNOWLEDGEMENTS

This work is partly supported by US-Japan collaboration, and JSPS KAKENHI 19K21877 and 19H04395.

REFERENCES

[1] A. Grassellino, "Overview of Progress in High Q and High G in Niobium Cavities", presented at the 19th Int. Conf. on RF Superconductivity (SRF'19), Dresden, Germany, June-July 2019, paper TUFUA2, unpublished.

[2] J. M. Köszegiet *et al.*, "A Combined Temperature and Magnetic Field Mapping System for SRF Cavities", in *Proc. 9th Int. Particle Accelerator Conf. (IPAC'18)*, Vancouver, Canada, Apr.-May 2018, pp. 1228-1231. doi:10.18429/JACoW-IPAC2018-TUZGBE5

[3] Y. Iwashita *et al.*, "R&D of Non-destructive Inspection System for SRF Cavities", in *Proc. 14th Int. Conf. on RF Superconductivity (SRF'09)*, Berlin and Dresden, Germany, September 2009, pp. 297-299.

[4] Y. Iwashita *et al.*, "High Density Mapping for Superconducting Cavities", in *Proc. 10th Int. Particle Accelerator Conf. (IPAC'19)*, Melbourne, Australia, May 2019, pp. 2860-2862. doi:10.18429/JACoW-IPAC2019-WEPRB025

[5] R. L. Geng *et al.*, "Preliminary Cryogenic Cold Test Results of the First 9-Cell LSF Shape Cavity", in *Proc. 12th Int. Particle Accelerator Conf. (IPAC'21)*, Campinas, Brazil, May 2021, pp. 2296-2299. doi:10.18429/JACoW-IPAC2021-TUPAB342

[6] R. H. Fowler and L. Nordheim, "Electron Emission in Intense Electric Fields", *Proc. R. Soc. London, Ser A*, vol. 119, p. 173, 1928. doi:10.1098/rspa.1928.0091

[7] E. L. Murphy and R. H. Good Jr., "Thermionic Emission, Field Emission and the Transition Region", *Phys. Rev.*, vol. 102, no. 6, p. 1464, 1956. doi:10.1103/PhysRev.102.1464